

Prestack depth migration with acoustic screen propagators

Lian-Jie Huang* and Ru-Shan Wu, Institute of Tectonics, University of California, Santa Cruz

Summary

We develop a prestack depth migration method for common-shot gathers using the wide-angle-screen and phase-screen propagators as recursive downward wave extrapolators. These screen propagators are acoustic one-way wave propagators carried out in the dual-domain (wavenumber-space domain). The proposed migration method takes into account lateral velocity and density variations and implements exactly the transversal Laplacian operators in the acoustic wave equation. It has fast computational speed due to the use of fast Fourier transform algorithm. Another advantage of the method is huge memory saving compared to finite-difference or ray tracing based methods. The phase-screen migration is also unconditionally stable. Because of these advantages, the screen prestack depth migration method may enable the large 3D prestack migration to be implemented within a reasonable CPU time on a supercomputer. The feasibility of the method is demonstrated by migrating synthetic data generated by a finite-difference algorithm.

Introduction

Prestack depth migration is an important and effective tool for imaging complex subsurface structures. Existing migration methods are implemented in either the time domain or the frequency domain. In the latter case, the propagation can be in the wavenumber domain or the wavenumber-space dual-domain. Prestack reverse-time migration is a time domain method in which wave fields are generally extrapolated by a finite-difference scheme (e.g. Chang and McMechan, 1990). Another kind of time domain methods is based on the Kirchhoff integral and ray tracing (e.g. Hu and McMechan, 1986). Finite-difference and ray tracing methods are both so time-consuming that the corresponding prestack migration methods are currently not realistic to large 3D imaging problems. Another problem of these methods is their requirements of huge computer memory size. The phase-shift migration developed by Gazdag (1978) is implemented in the frequency-wavenumber domain and has the attractive advantages such as exactly implementing the transversal Laplacian operators in the wave equation, unconditionally stability as well as fast computational speed benefited from using a fast Fourier transform (FFT) algorithm. However, the method uses a constant velocity of each depth interval and cannot handle lat-

eral velocity variations. The phase-shift plus interpolation (PSPI) was hence developed by Gazdag and Sguazzero (1984) as one way to handle lateral velocity variations. It is a dual-domain method. Several constant reference velocities are used in the PSPI to perform phase-shift migrations for each depth interval and the corresponding migration results are interpolated to yield the final migrated image. The PSPI would be very time-consuming for imaging large 3D complex structures because many reference velocities have to be selected for these cases. Another existing dual-domain migration method is the split-step Fourier migration introduced by Stoffa et al. (1990) for post-stack migration to take into account lateral velocity variations while retaining the advantages of the phase-shift migration.

The wide-angle-screen and phase-screen propagators are one-way wave propagators for acoustic waves in heterogeneous media. They are carried out in the dual-domain and have been recently used for modeling primary reflections (Wu and Huang, 1992, 1995; Wu et al. 1995). We use these propagators as recursive downward wave extrapolators from sources and receivers to develop a prestack depth migration method for common-shot gathers. The method takes into account lateral velocity variations as well as lateral density variations. It has fast computational speed due to the use of a FFT algorithm and requires much smaller computer memory size than time domain methods because it needs only to store the wave field at one depth level in a 3D medium rather than wave fields at all depth levels during the wave field extrapolation at each depth level. We first briefly present the formulation of the wide-angle-screen and phase-screen propagators and give the imaging condition. Numerical examples are then given to demonstrate the feasibility of the method. The application of the method to 3D cases is ongoing and the results will be presented in the near future.

Acoustic wide-angle-screen propagator

The wave equation for heterogeneous acoustic media is given by

$$\nabla \cdot \frac{1}{\rho} \nabla P + \frac{\omega^2}{\kappa} P = 0, \quad (1)$$

where P is the pressure, ρ is the medium density, $\kappa = \rho v^2$ is the bulk modulus of the medium with velocity v , and ω is the circular frequency. Under

the screen approximation, the interaction of heterogeneities within a thin-slab from depth z_i to z_{i+1} with the wave field is approximated by the interaction of the effective heterogeneities of a screen at z_{is} located at the center of the thin-slab (cf Figure 1 for the 2D case). We first discuss the case of the downward propagation from a source. Starting from equation (1), taking the de Wolf approximation and the screen approximation yields the dual-domain expression for the forward scattered pressure field $P_s(\mathbf{K}_T, z_{i+1})$ at the depth z_{i+1} (cf Wu and Huang 1995 for the formulation under the de Wolf approximation)

$$P_s(\mathbf{K}_T, z_{i+1}) = \frac{i}{2k_z} k^2 (z_{i+1} - z_i) e^{ik_z(z_{i+1} - z_{is})} \left\{ \int [\varepsilon_\kappa(\mathbf{x}_T, z_{is}) P_0(\mathbf{x}_T, z_{is})] e^{-i\mathbf{K}_T \cdot \mathbf{x}_T} d^2 \mathbf{x}_T \right. \\ \left. + \frac{i}{k} \hat{k} \cdot \int [\varepsilon_\rho(\mathbf{x}_T, z_{is}) \nabla P_0(\mathbf{x}_T, z_{is})] e^{-i\mathbf{K}_T \cdot \mathbf{x}_T} d^2 \mathbf{x}_T \right\}, \quad (2)$$

where

$$k_z = \sqrt{k^2 - K_T^2}, \quad (3)$$

$$\hat{k} = \frac{1}{k}(\mathbf{K}_T, k_z). \quad (4)$$

The dependence on ω has been and will be omitted in the following except otherwise explicitly indicated. In the above equations, \mathbf{K}_T denotes the transverse component of wavenumber and $k = \omega/v_0$ is the wavenumber where v_0 is the velocity of a background medium. \mathbf{x}_T is the horizontal component of the position vector \mathbf{x} . $\varepsilon_\kappa(\mathbf{x}_T, z_{is})$ and $\varepsilon_\rho(\mathbf{x}_T, z_{is})$ are respectively given by

$$\varepsilon_\kappa(\mathbf{x}_T, z_{is}) \equiv \frac{\kappa_0(z_{is})}{\kappa(\mathbf{x}_T, z_{is})} - 1, \quad (5)$$

$$\varepsilon_\rho(\mathbf{x}_T, z_{is}) \equiv \frac{\rho_0(z_{is})}{\rho(\mathbf{x}_T, z_{is})} - 1, \quad (6)$$

where ρ_0 and κ_0 are the density and bulk modulus of the background medium, respectively. The incident field $P_0(\mathbf{x}_T, z_{is})$ and its gradient $\nabla P_0(\mathbf{x}_T, z_{is})$ at the screen z_{is} are respectively calculated from the pressure field at z_i using the equations

$$P_0(\mathbf{x}_T, z_{is}) = \frac{1}{4\pi^2} \iint P(\mathbf{K}_T, z_i) e^{ik_z(z_{is} - z_i)} e^{i\mathbf{K}_T \cdot \mathbf{x}_T} d^2 \mathbf{K}_T \quad (7)$$

and

$$\nabla P_0(\mathbf{x}_T, z_{is}) = \frac{ik}{4\pi^2} \iint \hat{k} P(\mathbf{K}_T, z_i) e^{ik_z(z_{is} - z_i)} e^{i\mathbf{K}_T \cdot \mathbf{x}_T} d^2 \mathbf{K}_T. \quad (8)$$

The wave field at depth z_{i+1} is then given by

$$P(\mathbf{x}_T, z_{i+1}) = P_0(\mathbf{x}_T, z_{i+1}) + P_s(\mathbf{x}_T, z_{i+1}), \quad (9)$$

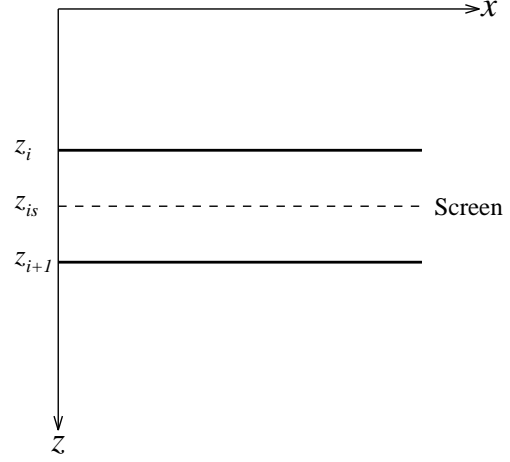


Figure 1: Schematic illustration of a screen model in the 2D case.

where $P_0(\mathbf{x}_T, z_{i+1})$ is obtained by

$$P_0(\mathbf{x}_T, z_{i+1}) = \frac{1}{4\pi^2} \iint P(\mathbf{K}_T, z_i) e^{ik_z(z_{i+1} - z_i)} e^{i\mathbf{K}_T \cdot \mathbf{x}_T} d^2 \mathbf{K}_T. \quad (10)$$

Therefore, the downward propagating wave field at depth z_{i+1} can be calculated from the downward propagating wave field at depth z_i using equations (2)–(10). This procedure can be written as

$$P(\mathbf{x}_T, z_{i+1}) = \mathcal{W} \{P(\mathbf{x}_T, z_i)\}, \quad (11)$$

where \mathcal{W} is called the acoustic wide-angle-screen propagator. The wide-angle feature of the propagator has also been numerically demonstrated (Wu and Huang, 1995).

For downward propagation of wave fields from common-shot gathers, the same procedure as above is used but the acoustic wide-angle-screen propagator \mathcal{W} is replaced by its complex conjugate.

Acoustic phase-screen propagator

Under the small-angle approximation, the wide-angle-screen propagator can be simplified to further speed up the computation speed (cf Wu and Huang, 1992, 1995 for the case of constant density media). In this case, the downgoing wave field is given by

$$P(\mathbf{K}_T, z_{i+1}) = e^{ik_z(z_{i+1} - z_{is})} \iint P_0(\mathbf{x}_T, z_{is}) e^{ik S_v(\mathbf{x}_T, z_{is})} e^{-i\mathbf{K}_T \cdot \mathbf{x}_T} d^2 \mathbf{x}_T, \quad (12)$$

where $P_0(\mathbf{x}_T, z_{is})$ is obtained from $P(\mathbf{x}_T, z_i)$ using equation (7) and S_v is defined by

$$S_v(\mathbf{x}_T, z_{is}) \equiv \frac{1}{2}(z_{i+1} - z_i) [\varepsilon_\kappa(\mathbf{x}_T, z_{is}) - \varepsilon_\rho(\mathbf{x}_T, z_{is})]. \quad (13)$$

Utilizing equations (12) and (7) and taking the inverse Fourier transform over \mathbf{K}_T , the downward propagating wave field at depth z_{i+1} is extrapolated from the wave field at depth z_i . This procedure for downward propagation of wave fields from a source can be written as

$$P(\mathbf{x}_T, z_{i+1}) = \mathcal{P} \{P(\mathbf{x}_T, z_i)\} , \quad (14)$$

where \mathcal{P} is termed the acoustic phase-screen propagator. Its complex conjugate is the acoustic phase-screen backward propagator for wave fields from common-shot gathers.

For the case of constant density, equation (13) can be written as

$$S_v(\mathbf{x}_T, z_{is}) = \frac{1}{2}(z_{i+1} - z_i) \left\{ \left[\frac{v_0(z_{is})}{v(\mathbf{x}_T, z_{is})} \right]^2 - 1 \right\} . \quad (15)$$

Under the approximation of $[v_0(z_{is})/v(\mathbf{x}_T, z_{is}) + 1] \approx 2$, equation (15) becomes

$$S_v(\mathbf{x}_T, z_{is}) \approx (z_{i+1} - z_i) \left[\frac{v_0(z_{is})}{v(\mathbf{x}_T, z_{is})} - 1 \right] . \quad (16)$$

Then the corresponding phase-shift term in equation (12) is the same as that used in the split-step Fourier migration method (Stoffa, et al., 1990).

Imaging condition

Let $P_+(x, y, z; \omega)$ be the downgoing wave field propagating from a point source and $P_-(x, y, z; \omega)$ be the upgoing wave field backpropagating from a common-shot gather. We use the imaging condition given by (Mittet et al. (1995))

$$M_S(x, y, z) = - \int i\omega P_+(x, y, z; \omega) P_-^*(x, y, z; \omega) d\omega , \quad (17)$$

where “*” denotes the complex conjugate. The final migrated image for common-shot gathers is

$$M(x, y, z) = \sum_{S=1}^{N_{shot}} M_S(x, y, z) , \quad (18)$$

where N_{shot} is the total number of shots.

Numerical examples

A finite-difference scheme solving the acoustic wave equation was used to generate synthetic data for a model defined on a 512×200 lattice with a grid spacing of $5m$ in the horizontal and vertical directions (cf Figure 2). The pressure sources with a Ricker’s time history were located at grid sites (128, 1), (192, 1), (256, 1), (320, 1), and (384, 1), as indicated by stars in Figure 2. The Ricker’s time history has a dominant frequency $10Hz$, an amplitude 1.0 and a time

delay $0.2s$. Receivers were put at all grid points at the upper boundary of the model. In the following migration examples, each trace of seismograms has 512 samples with a time sample interval $4ms$. The frequency range used in migration is $0-20Hz$ with 40 frequency components. A cosine taper with a length of 20 grid points was applied at the left and right boundaries of the model to eliminate the boundary effects. In the first example, the velocities and densities of the 3 layers of the model are $v_1 = 2200m/s$, $v_2 = 2100m/s$, $v_3 = 2200m/s$, $\rho_1 = 1.65g/cm^3$, $\rho_2 = 1.50g/cm^3$, $\rho_3 = 1.65g/cm^3$, respectively. Hence $\kappa_1/\kappa_2 = 1.21$ and $\rho_1/\rho_2 = 1.10$. The wide-angle-screen migration and the phase-screen migration were respectively performed for each common-shot gather. The final migrated images are displayed in Figure 3(a) and (b), respectively. Both interfaces are well migrated by both methods.

Next is a constant density example. The velocities of the 3 layers of the model are $v_1 = 2572m/s$, $v_2 = 2100m/s$, $v_3 = 2572m/s$, respectively. The densities of the 3 layers are all $1.50g/cm^3$. Hence $\kappa_1/\kappa_2 = 1.50$ and $\rho_1/\rho_2 = 1.0$. The corresponding migrated images are shown in Figure 4.

The above computations were made on a SUN SPARCstation 4. The average CPU time per frequency component is 6.7 seconds for the wide-angle-screen migration and 4.7 seconds for the phase-screen migration. The efficiency of the phase-screen migration can be further improved by using a larger depth interval because of its unconditionally stability.

Conclusions

We have developed an acoustic prestack depth migration method using the wide-angle-screen and phase-screen propagators. The method is implemented in the dual-domain and has advantages of fast computation speed and less computer memory size requirements. It has flexibility of selecting an interested frequency range for migration. The phase-screen migration method is also unconditionally stable. Numerical examples show that the method can properly take into account the lateral velocity and density variations. The computation for each frequency can be made independently and, therefore, the migrations for different frequencies can be performed in parallel.

Acknowledgements

We would like to thank X.-B. Xie for helpful discussion. The support from the ACTI project of UCSC granted from the United States Department of Energy administered by the Los Alamos National Laboratory and the support from the W. M. Keck Foundation are

acknowledged. The University of California at Santa Cruz, Institute of Tectonics contribution number 300.

References

Chang, W.-F., and McMechan, G. A., 1990, 3D acoustic prestack reverse-time migration: *Geophys. Prosp.*, **38**, 737–755.

Gazdag, J., 1978, Wave equation migration with the phase-shift method: *Geophysics*, **43**, 1342–1351.

Gazdag, J., and Sguazzero, P., 1984, Migration of seismic data by phase shift plus interpolation: *Geophysics*, **49**, 124–131.

Hu, L.-Z., and McMechan, G. A., 1986, Migration of VSP data by ray equation extrapolation in 2-D variable velocity media: *Geophys. Prosp.*, **34**, 704–734.

Mittet, R., Sollie, R., and Hokstad, K., 1995, Prestack depth migration with compensation for absorption and dispersion: *Geophysics*, **60**, 1485–1494.

Stoffa, P. L., Fokkema, J. T., de Luna Freire, R. M., and Kessinger, W. P., 1990, Split-step Fourier migration: *Geophysics*, **55**, 410–421.

Wu, R.-S., and Huang, L.-J., 1992, Scattered field calculation in heterogeneous media using the phase-screen propagator: 62nd Ann. Internat. Mtg., Soc. Expl. Geophys., Expanded Abstracts, 1289–1292.

Wu, R.-S., and Huang, L.-J., 1995, Reflected wave modeling in heterogeneous acoustic media using the de Wolf approximation: *in* S. Hassanzadeh, Editor, *Mathematical Methods in Geophysical Imaging III*, Proc. SPIE **2571**, 176–186.

Wu, R.-S., Huang, L.-J., and Xie, X.-B., 1995, Backscattered wave calculation using the de Wolf approximation and a phase-screen propagator: 65th Ann. Internat. Mtg., Soc. Expl. Geophys., Expanded Abstracts, 1293–1296.

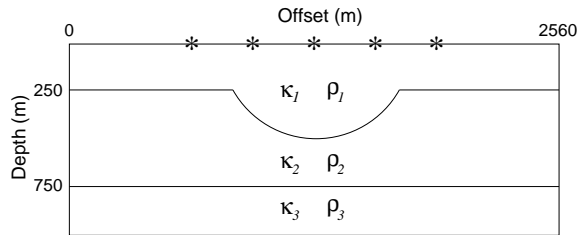


Figure 2: Illustration of a model used for migration. The stars represent the positions of pressure sources.

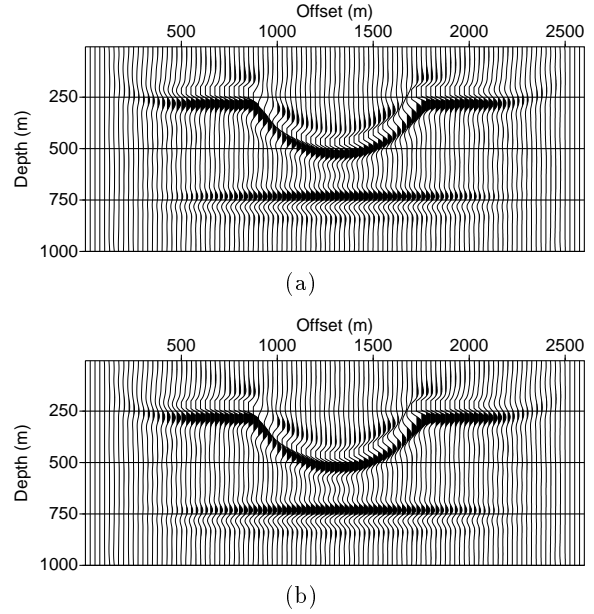


Figure 3: Prestack depth migration results using the wide-angle-screen propagator (a) and the phase-screen propagator (b). $\kappa_1/\kappa_2 = 1.21$, $\kappa_3 = \kappa_1$, $\rho_1/\rho_2 = 1.10$, $\rho_3 = \rho_1$.

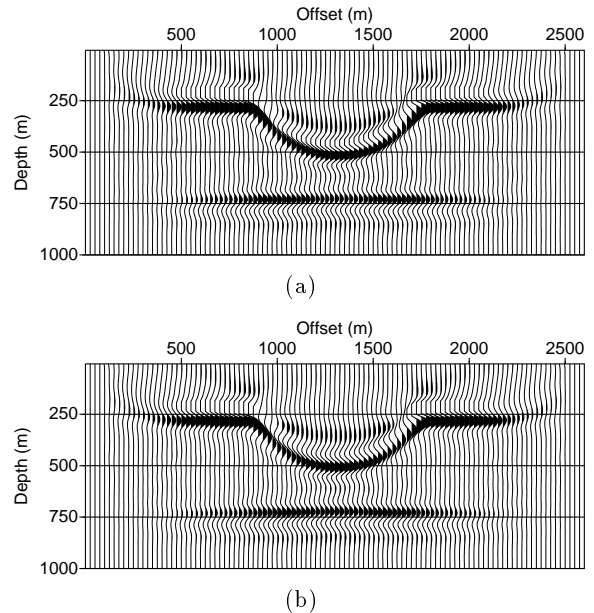


Figure 4: Prestack depth migration results using the wide-angle-screen propagator (a) and the phase-screen propagator (b). $\kappa_1/\kappa_2 = 1.50$, $\kappa_3 = \kappa_1$, $\rho_1 = \rho_2 = \rho_3 = 1.50$.